

Tuning the piezoelectric and mechanical properties of the AlN system via alloying with YN and BN

Sukriti Manna¹, Geoff L. Brennecke², Vladan Stevanović² and Cristian V. Ciobanu^{1*}

¹*Dept. of Mechanical Engineering, Colorado School of Mines, Golden, Colorado 80401*

²*Dept. of Metallurgical and Materials Engineering, Colorado School of Mines, Golden, Colorado 80401*

Abstract: Recent advances in microelectromechanical systems often require multifunctional materials, which are designed so as to optimize more than one property. Using density functional theory calculations for alloyed nitride systems, we illustrate how co-alloying a piezoelectric material (AlN) with different nitrides helps tune both its piezoelectric and mechanical properties simultaneously. Wurtzite AlN-YN alloys display increased piezoelectric response with YN concentration, accompanied by mechanical softening along the crystallographic c direction. Both effects increase the electromechanical coupling coefficients relevant for transducers and actuators. Resonator applications, however, require superior stiffness, thus leading to the need to decouple the increased piezoelectric response from a softened lattice. We show that co-alloying of AlN with YN and BN results in improved elastic properties while retaining most of the piezoelectric enhancements from YN alloying. This finding may lead to new avenues for tuning the design properties of piezoelectrics through composition-property maps.

Keywords: piezoelectricity, electromechanical coupling, density functional theory, co-alloying

* To whom correspondence may be addressed, electronic mail: cciobanu@mines.edu

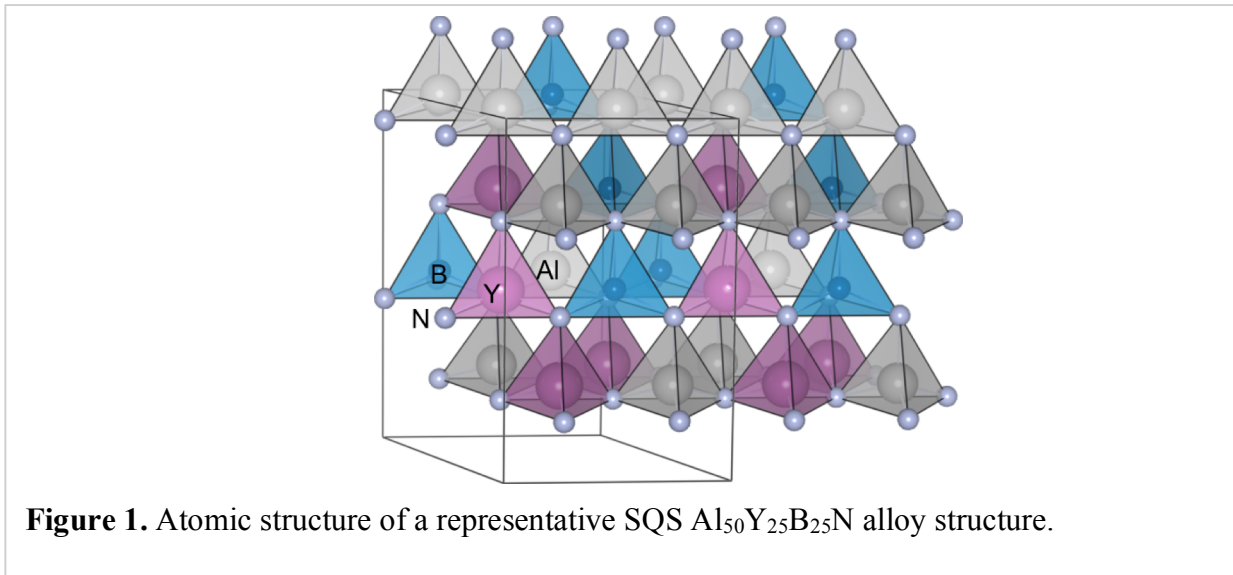
Recent technological advances in microelectromechanical systems require materials to be more efficiently designed, often leading to optimization of more than one property^{1, 2}. An electromechanical (piezoelectric) material requires the best piezoelectric coefficient, while materials for damping high mechanical loads require the high stiffness moduli.^{3, 4} The high stiffness value is also associated with thermal stability, enabling the use of these materials over a large temperature range.⁵ Pseudo-binary alloys, i.e. solid solutions between two compounds, have been extensively investigated for use in electromechanical applications.⁶⁻¹⁰ Most of these alloys have large miscibility gaps, making them less appealing for applications where mechanical stability is an important figure of merit. Current processing techniques allow for fabricating pseudo-binary alloys in which one can seek a given functionality by, e.g., changing composition so as to optimize piezoelectric coefficients, stiffness, electromechanical coupling constants, or bandgap to desired values. However, achieving optimal or desired values for more than one such property is challenging since optimizing one property often changes another towards undesirable values. In such cases, more degrees of freedom may help create a framework in which advanced materials can be optimized for multiple functionalities. In this article, we focus on a piezoelectric system to show that alloying with than one compound enables us to tune two properties, specifically, the piezoelectric coefficient and the mechanical stiffness.

With the discovery of the anomalously large increase in the piezoelectric moduli of wurtzite AlN when alloyed with ScN¹¹ or YN,^{9, 12} AlN-based alloys have received a lot of attention as materials for improved telecommunications, sensors, and surface acoustic wave devices.^{13, 14} The origin of the enhanced piezoelectricity was revealed to be an intrinsic effect of alloying, as opposed to textural or microstructural effects,⁶ with the obvious implication that controlling the piezoelectric enhancement can be done mainly by increasing composition of YN or ScN. However, such alloying softens the material significantly,⁶ which actually makes the material *less* attractive for resonant applications for which k^2Q is a common figure of merit,¹⁵ where k is an electromechanical coupling coefficient and Q is a quality factor that is inversely proportional to mechanical dissipation.¹⁵ It is therefore desirable to control the mechanical properties as well, which could in principle be achieved by alloying with other species.

Herein, we focus on AlN-YN alloys and advance the premise that further alloying this system with BN can increase the elastic constants of the material, thus leading to new avenues for piezoelectric design based on precise control YN and BN compositions. The choice for YN is

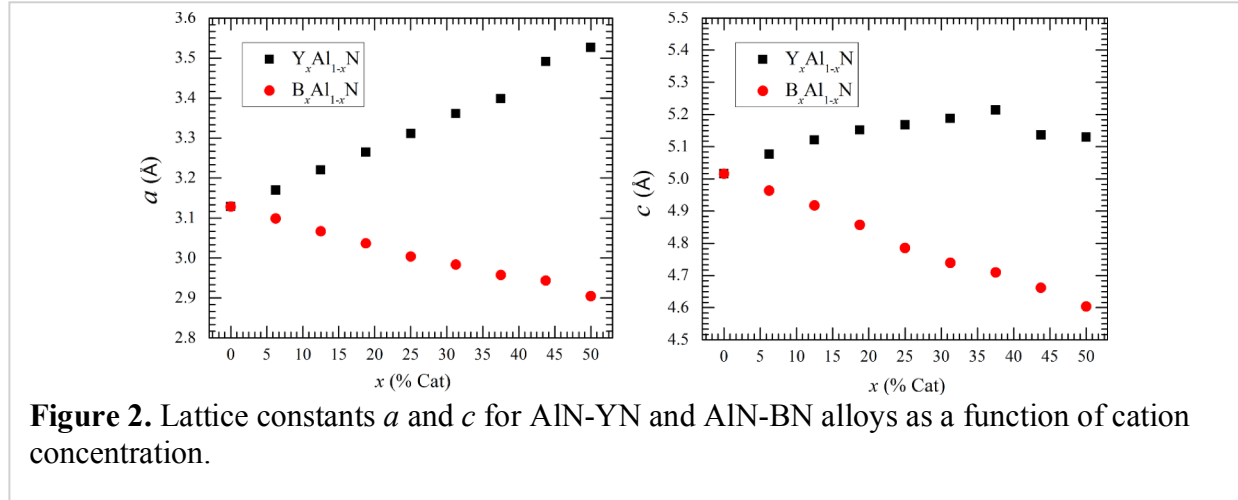
motivated by the scarcity of literature reports on AlN-YN alloys,^{12, 16} and by the fact that Y can be a less expensive alternative for Sc. While the elastic stiffening of AlN co-alloyed with YN and BN would be enabled by the presence of shorter and stiffer B–N bonds, the effect of alloying with BN on the piezoelectric properties is presently unknown. Using density functional theory (DFT), we have found that the presence of BN, by itself, indeed leads to increases in the relevant elastic constant C_{33} , but does not change the piezoelectric coefficient e_{33} significantly. Furthermore, we have uncovered the combined effect of alloying with YN and BN on the properties of the AlN system for total alloying concentrations up to 50 at. %. The addition of BN to AlN-YN alloys counters to some extent the piezoelectric enhancement obtained via YN alloying, but increases the elastic modulus. Overall, the alloying of AlN with BN and YN leads to a high degree of control over the piezoelectric and elastic properties of the resulting alloy, and therefore over the coupling coefficients and various figures of merit commonly used in piezoelectric device design.

To assess the changes in elastic and piezoelectric properties driven by different levels of YN and BN in $\text{Al}_{1-x-y}\text{Y}_x\text{B}_y\text{N}$ alloys, we first performed DFT relaxations of atomic positions and lattice constants using the VASP package,¹⁷ with projector augmented waves¹⁸ in the generalized gradient approximation (GGA) using the Perdew-Burke-Ernzerhof exchange-correlation functional.¹⁹ We introduced an on-site Coulomb interaction (parameter $U = 3$ eV) for the yttrium

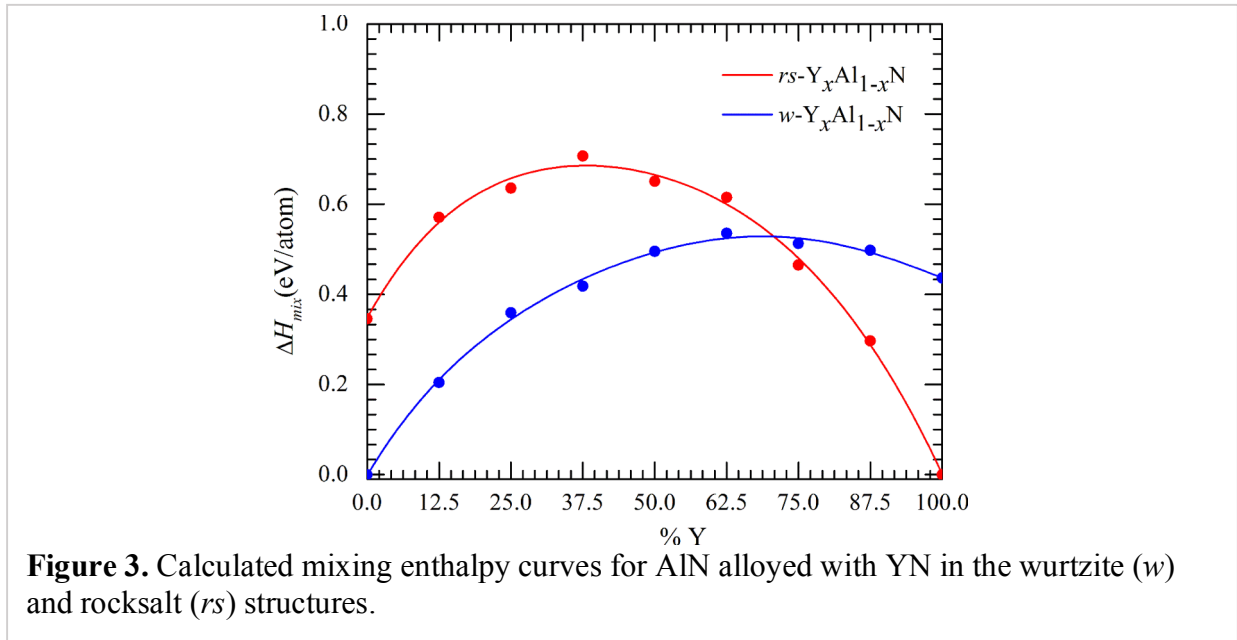


3 d states.²⁰ The parent structure is wurtzite AlN, in which Al is substituted with Y and B in the desired amounts. Supercells with 32 atoms are simulated using special quasirandom structures (SQS)²¹ (Fig. 1), whose pair correlation functions are the same as those of random alloys up to

second-nearest neighbors. A plane wave cutoff energy of 500 eV was used; the energy tolerance stopping criteria were 10^{-8} and 10^{-7} for the electronic and ionic convergence, respectively. A $5 \times 5 \times 3$ Monkhorst–Pack^{22, 23} k -point mesh was used to sample the Brillouin zone, resulting in 38 irreducible k -points. The SQS supercells have been relaxed to obtain equilibrium lattice constants for all compositions studied. Due to the variability of atomic-scale environments in the SQS



supercells,⁸ we performed five calculations at each composition and used them to average the the properties, including the lattice constants, which are plotted in Fig. 2. Our DFT calculations revealed that YN is miscible in AlN up to $\sim 72\%$ YN concentration, above which the wurtzite phase becomes unstable towards rocksalt structure formation (Fig. 3).



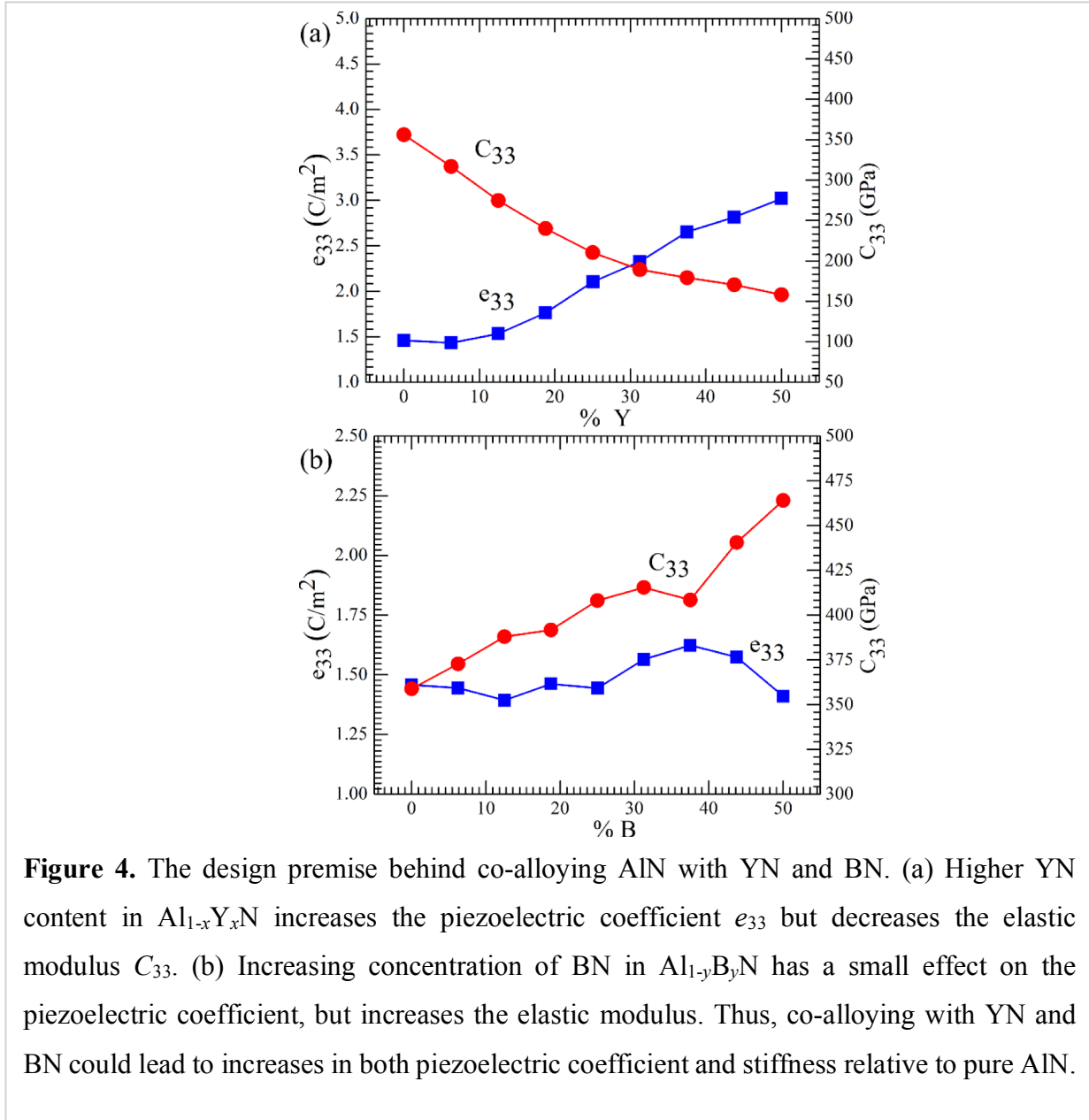
The piezoelectric charge coefficient e_{33} is evaluated at each Y (x) and B (y) composition via

$$e_{33} = e_{33}^{clamped-ion} + \frac{4eZ^*}{\sqrt{3}a_0^2} \frac{du}{d\varepsilon}$$

where $e_{33}^{clamped-ion}$ is the clamped ion contribution to e_{33} ,^{23, 24} e is the electron charge, Z^* is the axial component of the dynamical Born effective charge tensor, a_0 is the equilibrium lattice constant, and $du/d\varepsilon$ is the sensitivity of the internal parameter u to strains along the crystallographic c -axis. The elastic constants were computed by finite differences between the energies of the lattices subjected to small applied strains.²⁵

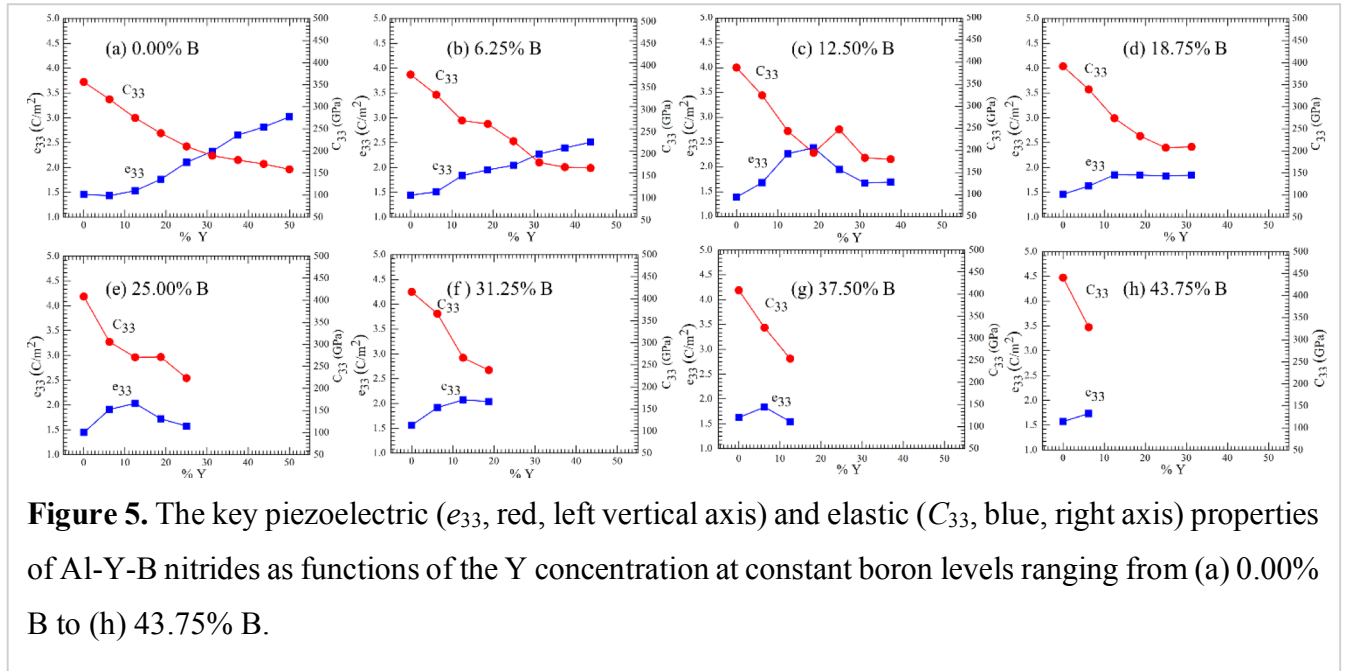
Figure 4 shows the effects of separate BN and YN alloying on the properties of AlN. As seen in Fig. 4 (a) the piezoelectric coefficient e_{33} increases with Y concentration up to 50%, while the elastic constant C_{33} decreases; this is consistent with previous works on the similar AlN-ScN

system.^{6, 8} Figure 4 (b) shows that alloying with BN alone increases the elastic modulus, which is consistent to another report.²⁶ Interestingly, we also note that substituting B for Al does not alter the piezoelectric coefficient significantly up to concentrations of 50% B. Based on these results, we have set out to analyze how co-alloying with both YN and BN changes properties, with the



purpose of identifying composition regimes where the piezoelectric coefficient increases while the elastic modulus does not decrease to the same extent as in the case of alloying with Y alone.

Figure 5 shows the variation of e_{33} and C_{33} with the Y concentration x , at a fixed level of B doping, y (such that $x+y \leq 50\%$). The data points in Fig. 5 represent averages over SQS



configurations. Other properties (i.e., e_{31} and C_{11}) are shown in Fig. SM-1 as functions of x and y . Our starting premise that the presence of boron can mitigate or control the decrease in elastic modulus C_{33} brought about by Y alloying while still retaining some increase of the piezoelectric coefficient is borne out by the results in Fig. 5. For example, going from 0% B in $\text{Al}_{50}\text{Y}_{50}\text{N}$ to 18.75% B concentration in $\text{Al}_{50}\text{Y}_{31.25}\text{B}_{18.75}\text{N}$ results in a ~ 50 MPa increase of the elastic constant C_{33} with $\sim 33\%$ decrease in the piezoelectric coefficient. For ease of reference, some of the results shown in Fig. 5 are also tabulated in Table I.

Table I. Comparison between the properties of some of the Al-Y-B nitrides computed in this work and those of three commercial piezoelectrics.

Material	e_{33} (C/m ²)	C_{33} (GPa)	d_{33} (pC/N)	k_{33}^2
PZT-7A, Ref. ²⁷	9.50	131	153	0.67
PZT-4, Ref. ²⁷	13.84	113	225	0.35
K _{0.5} Na _{0.5} NbO ₃ , Ref. ^{28, 29}	4.14	104	80, 130	0.51
<i>this work:</i>				
AlN	1.46	353	5	0.12
Al ₅₀ Y ₅₀ N	3.02	158	38	0.57
Al ₅₀ Y _{43.75} B _{6.25} N	2.51	161	22	0.47
Al ₅₀ Y _{37.50} B _{12.50} N	1.70	180	13	0.27
Al ₅₀ Y _{31.25} B _{18.75} N	1.85	209	13	0.27
Al ₅₀ Y ₂₅ B ₂₅ N	1.58	223	13	0.20
Al ₅₀ Y _{18.75} B _{31.25} N	1.93	238	13	0.26
Al ₅₀ Y _{12.5} B _{37.50} N	1.54	253	9	0.17
Al ₅₀ Y _{6.25} B _{43.75} N	1.73	328	8	0.17
Al ₅₀ B ₅₀ N	1.34	470	3	0.08

Next, we discuss the electromechanical coupling coefficients resulting from co-alloying of AlN with YN and BN. These coefficients are key parameters in designing transducers for energy harvesting and sensing applications.^{5, 30} Applications such as pressure sensors, accelerometers, and gyroscopes commonly require the piezoelectric medium to operate in the longitudinal length mode,³¹ for which the relevant coupling coefficient is

$$k_{33}^2 = \frac{e_{33}^2}{\epsilon_{33} C_{33} + e_{33}^2}$$

where ϵ_{33} is the 33 component of the dielectric tensor. The static dielectric constants vary by only 10 %, approximately, from their value at $x=12.5\%$ (Fig. SM-2) for the entire range of equimolar Y-B doping (i.e., $x \leq 25\%$ in Al_{1-2x}Y_xB_xN), so a constant value of $\epsilon_{33} = 5.0$ was assumed in computing the coupling coefficients. High k_{33}^2 coupling factor corresponds to transducers with better axial resolution, broader bandwidth, and higher sensitivity.³² Actuators based on cantilevers operate in the transverse length mode (bending),^{30, 33} for which the relevant coupling coefficient is

$$k_{31}^2 = \frac{e_{31}^2}{\varepsilon_{33} C_{11} + e_{31}^2},$$

where e_{31} and C_{11} are components of the piezoelectric and elastic tensor, respectively. The two coupling coefficients are plotted in Fig. 6 (a,b), for the range of Y and B concentrations considered. High coupling constants require large piezoelectric coefficients and low elastic moduli. Increasing the amount of Y in the system increases the piezoelectric and coupling coefficients but softens the system elastically,⁶ which is true for both coupling modes addressed here.

The two coupling coefficients exhibit similar trends (Fig. 6), with larger values achieved for higher Y concentrations. However, variations of k_{31}^2 are significantly smaller, and larger values can also be achieved using equiatomic Y:B alloys. With the piezoelectric and elastic tensor components obtained from DFT calculations, it is useful to compare some of the properties of the co-alloyed AlN system with those of known piezoelectrics. Table I, which also includes the longitudinal piezoelectric modulus⁸ d_{33} , shows the properties of three well-known piezoelectrics in comparison with a few selected alloy compositions computed here (for completeness, piezoelectric moduli are also plotted in Fig. SM-3 for the entire range of compositions used). Direct inspection shows that AlN co-alloyed with Y and B can achieve parameters comparable to those of commercial piezoelectrics. More importantly, the simultaneous enhancement of e_{33} and C_{33} in comparison to the pure AlN values can be seen for boron levels of up $y = 25\%$, illustrating that co-alloying with different species represents a valuable route for simultaneously engineering the piezoelectric and the elastic properties of a parent wurtzite structure such as that of AlN.

The results presented here could carry over to other parent phases and alloying phases as well, provided that each alloying agent offers a clear advantage in terms of engineering one specific property. In our case, YN leads to increasing the piezoelectric coefficient and BN leads to increasing the stiffness. The use of both YN and BN offers intrinsic, simultaneous control over the mechanical and piezoelectric properties of the Al-Y-B-N system, even though the maximal value for each individual parameter can be achieved in the presence of only one dopant.

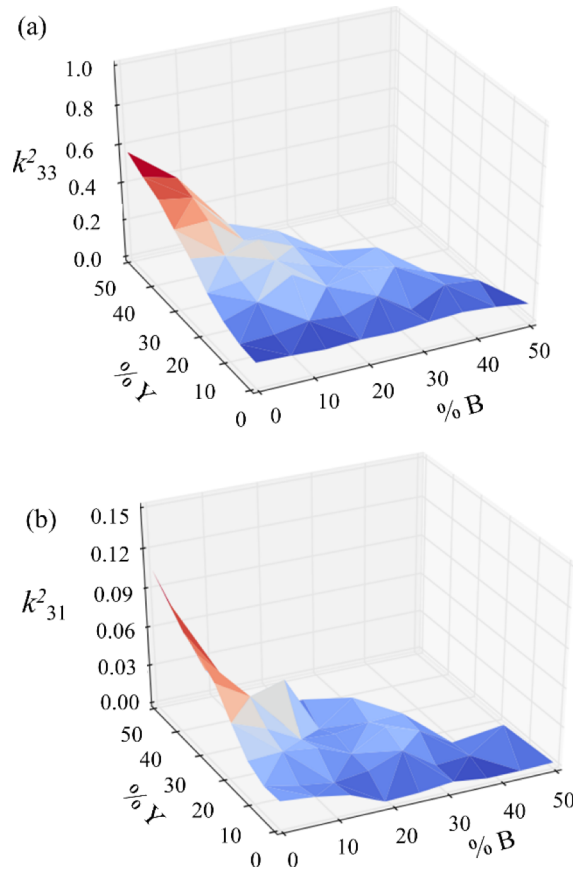


Figure 6. The coupling constants k_{33}^2 and k_{31}^2 as functions of the Y and B concentrations in $\text{Al}_{1-x-y}\text{Y}_x\text{B}_y\text{N}$ with at least 50% Al.

Acknowledgment. The authors gratefully acknowledge the support of the National Science Foundation through Grant No. DMR-1534503. The calculations were performed using the high-performance computing facilities of the Golden Energy Computing Organization.

SUPPLEMENTARY MATERIAL

1. Variations of e_{31} and C_{11} with Y and B composition

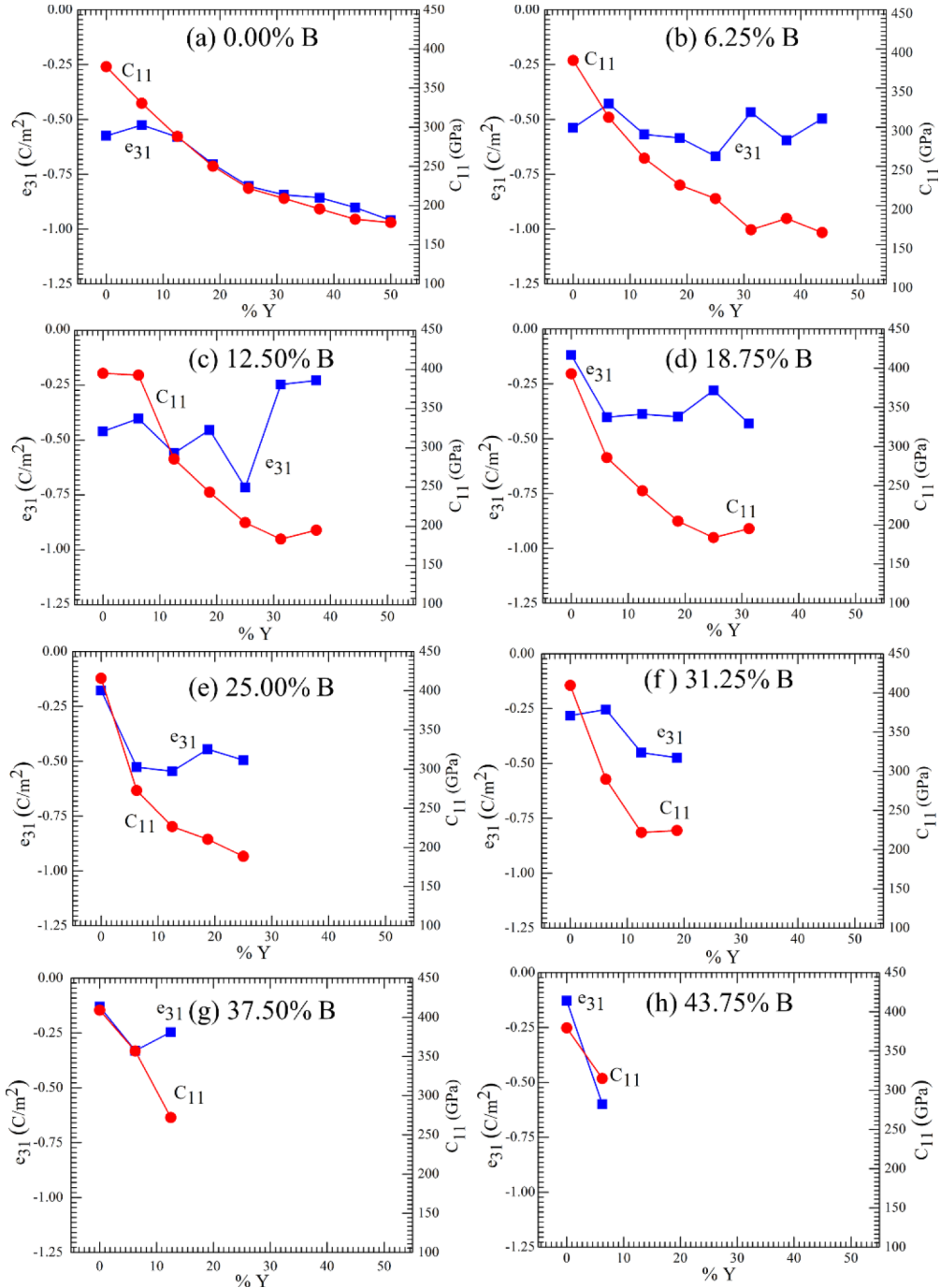
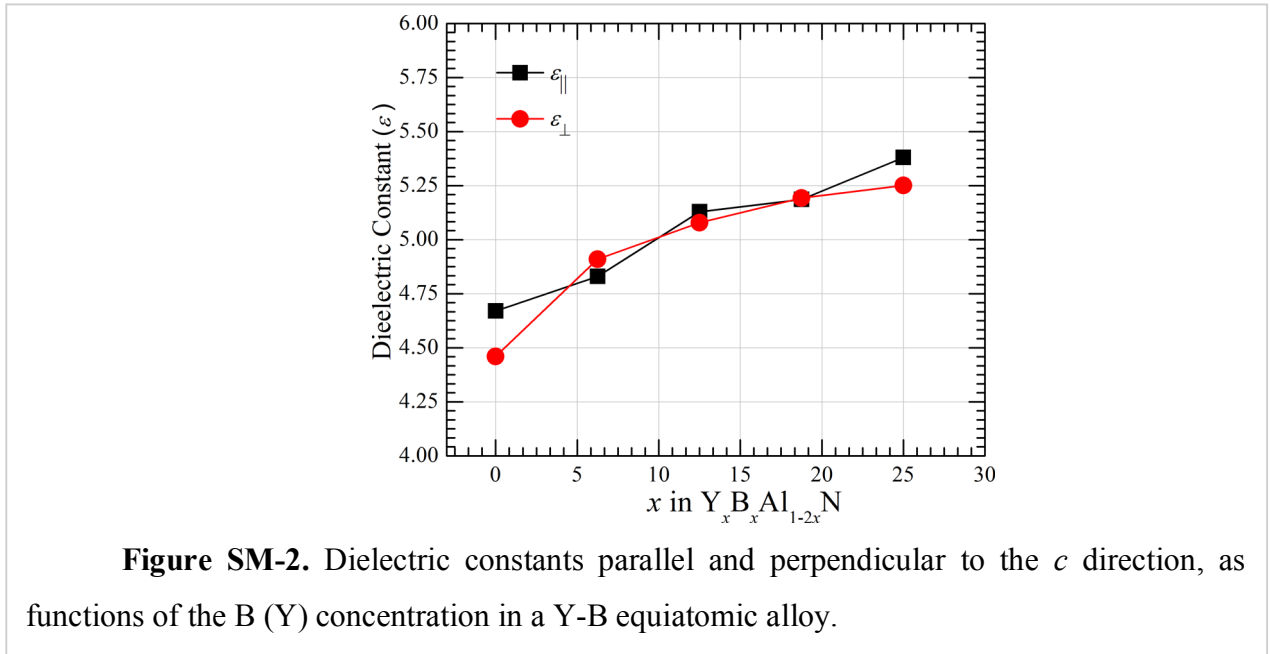


Figure SM-1. Piezoelectric coefficient e_{31} and elastic modulus C_{11} as functions of Y and B concentrations.

In the main text, we discussed the e_{33} and C_{33} coefficients which are important for thin film bulk acoustic wave resonators (TFBARs) in sensor, transducer, and actuator applications.³³ When using piezoelectric materials in the bending mode,³⁴⁻³⁶ e.g., contracting actuators, tube actuators, or bending actuators, the important piezoelectric and stiffness coefficients are e_{31} and C_{11} . For completeness, these are plotted in Fig. SM-1 as a function of the Y concentration, at fixed boron levels.

2. Static dielectric constants

The determination of the electromechanical coupling coefficients requires the computation of the dielectric constant, as described in the main text. We have used the VASP package to calculate the components of the static dielectric tensor, using density functional perturbation theory (DFPT) calculation; this provided the dielectric constant tensor that includes the electronic contribution as well as the ionic contribution.^{37, 38} The components parallel and perpendicular to the c axis are shown in Fig. SM-2, as a function of concentration for equiatomic Y-B alloys.



3. Piezoelectric moduli as functions of composition

The piezoelectric moduli are calculated from⁸

$$d_{33} = \frac{e_{33}(C_{11} + C_{12}) - 2e_{31}C_{12}}{(C_{11} + C_{12})C_{33} - 2C_{13}^2},$$

$$d_{31} = \frac{e_{31}C_{33} - e_{33}C_{13}}{(C_{11} + C_{12})C_{33} - 2C_{13}^2}$$

and are plotted in Fig. SM-3.

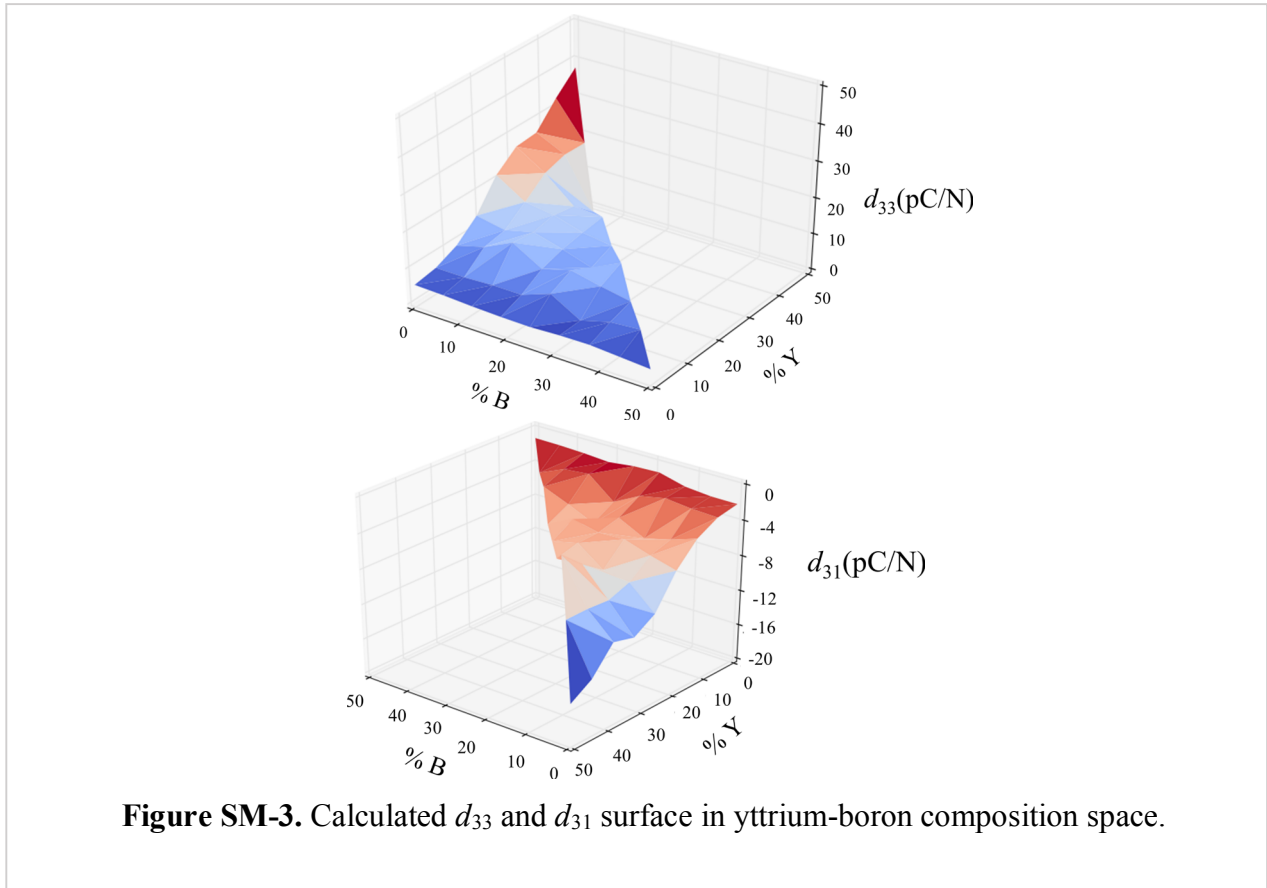


Figure SM-3. Calculated d_{33} and d_{31} surface in yttrium-boron composition space.

References

1. S.-H. Park, H. B. Lee, S. M. Yeon, J. Park and N. K. Lee, *Flexible and Stretchable Piezoelectric Sensor with Thickness-Tunable Configuration of Electrospun Nanofiber Mat and Elastomeric Substrates*, ACS Applied Materials & Interfaces **8**, 24773-24781 (2016).
2. C. Pang, G.-Y. Lee, T.-i. Kim, S. M. Kim, H. N. Kim, S.-H. Ahn and K.-Y. Suh, *A Flexible and Highly Sensitive Strain-Gauge Sensor Using Reversible Interlocking of Nanofibres*, Nature materials **11**, 795-801 (2012).

3. J. A. Rogers, T. Someya and Y. Huang, *Materials and Mechanics for Stretchable Electronics*, *Science* **327**, 1603-1607 (2010).
4. K. Uchino, *Materials Issues in Design and Performance of Piezoelectric Actuators: An Overview*, *Acta Materialia* **46**, 3745-3753 (1998).
5. S. Trolier-McKinstry and P. Muralt, *Thin Film Piezoelectrics for Mems*, *Journal of Electroceramics* **12**, 7-17 (2004).
6. F. Tasnádi, B. Alling, C. Höglund, G. Wingqvist, J. Birch, L. Hultman and I. A. Abrikosov, *Origin of the Anomalous Piezoelectric Response in Wurtzite Sc XAl 1– XN Alloys*, *Physical review letters* **104**, 137601 (2010).
7. S.-B. Kim, H. Park, S.-H. Kim, H. C. Wickle, J.-H. Park and D.-J. Kim, *Comparison of Mems Pzt Cantilevers Based on D_{31} and D_{33} Modes for Vibration Energy Harvesting*, *Journal of microelectromechanical systems* **22**, 26-33 (2013).
8. M. A. Caro, S. Zhang, T. Riekkinen, M. Ylilampi, M. A. Moram, O. Lopez-Acevedo, J. Molarius and T. Laurila, *Piezoelectric Coefficients and Spontaneous Polarization of ScAlN*, *Journal of Physics: Condensed Matter* **27**, 245901 (2015).
9. P. Mayrhofer, H. Riedl, H. Euchner, M. Stöger-Pollach, P. Mayrhofer, A. Bittner and U. Schmid, *Microstructure and Piezoelectric Response of YxAl 1– Xn Thin Films*, *Acta Materialia* **100**, 81-89 (2015).
10. C. Tholander, J. Birch, F. Tasnádi, L. Hultman, J. Palisaitis, P. Å. Persson, J. Jensen, P. Sandström, B. Alling and A. Žukauskaitė, *Ab Initio Calculations and Experimental Study of Piezoelectric YX in 1– XN Thin Films Deposited Using Reactive Magnetron Sputter Epitaxy*, *Acta Materialia* **105**, 199-206 (2016).
11. M. Akiyama, T. Kamohara, K. Kano, A. Teshigahara, Y. Takeuchi and N. Kawahara, *Enhancement of Piezoelectric Response in Scandium Aluminum Nitride Alloy Thin Films Prepared by Dual Reactive Cosputtering*, *Advanced Materials* **21**, 593-596 (2009).
12. A. Zukauskaitė, C. Tholander, J. Palisaitis, P. O. A. Persson, V. Darakchieva, N. Ben Sedrine, F. Tasnadi, B. Alling, J. Birch and L. Hultman, *YxAl 1– Xn Thin Films*, *Journal of Physics D-Applied Physics* **45** (2012).
10.1088/0022-3727/45/42/422001
13. G. Piazza, V. Felmetger, P. Muralt, R. H. Olsson III and R. Ruby, *Piezoelectric Aluminum Nitride Thin Films for Microelectromechanical Systems*, *MRS bulletin* **37**, 1051-1061 (2012).
14. Y. Zhang, W. Zhu, D. Zhou, Y. Yang and C. Yang, *Effects of Sputtering Atmosphere on the Properties of C-Plane ScAlN Thin Films Prepared on Sapphire Substrate*, *Journal of Materials Science: Materials in Electronics* **26**, 472-478 (2015).

15. R. R. Syms, H. Zou and P. Boyle, *Mechanical Stability of a Latching Mems Variable Optical Attenuator*, Journal of microelectromechanical systems **14**, 529-538 (2005).
16. C. Tholander, I. A. Abrikosov, L. Hultman and F. Tasnadi, *Volume Matching Condition to Establish the Enhanced Piezoelectricity in Ternary (Sc,Y)(0.5)(Al,Ga,in)(0.5)N Alloys*, Physical Review B **87** (2013).
10.1103/PhysRevB.87.094107
17. G. Kresse and J. Furthmüller, *Efficiency of Ab-Initio Total Energy Calculations for Metals and Semiconductors Using a Plane-Wave Basis Set*, Computational Materials Science **6**, 15-50 (1996).
18. J. P. Perdew, K. Burke and M. Ernzerhof, *Generalized Gradient Approximation Made Simple*, Physical review letters **77**, 3865 (1996).
19. G. Kresse and D. Joubert, *From Ultrasoft Pseudopotentials to the Projector Augmented-Wave Method*, Physical Review B **59**, 1758 (1999).
20. M. Barsukova, N. V. Izarova, R. N. Biboum, B. Keita, L. Nadjo, V. Ramachandran, N. S. Dalal, N. S. Antonova, J. J. Carbó and J. M. Poblet, *Polyoxopalladates Encapsulating Yttrium and Lanthanide Ions, [Xiiipdii12 (Asph) 8o32] 5-(X= Y, Pr, Nd, Sm, Eu, Gd, Tb, Dy, Ho, Er, Tm, Yb, Lu)*, Chemistry—A European Journal **16**, 9076-9085 (2010).
21. A. Van de Walle, P. Tiwary, M. De Jong, D. Olmsted, M. Asta, A. Dick, D. Shin, Y. Wang, L.-Q. Chen and Z.-K. Liu, *Efficient Stochastic Generation of Special Quasirandom Structures*, Calphad **42**, 13-18 (2013).
22. H. J. Monkhorst and J. D. Pack, *Special Points for Brillouin-Zone Integrations*, Physical Review B **13**, 5188 (1976).
23. D. Vanderbilt, *Berry-Phase Theory of Proper Piezoelectric Response*, Journal of Physics and Chemistry of Solids **61**, 147-151 (2000).
24. F. Bernardini, V. Fiorentini and D. Vanderbilt, *Spontaneous Polarization and Piezoelectric Constants of Iii-V Nitrides*, Physical Review B **56**, R10024 (1997).
25. B. Narayanan, I. E. Reimanis, E. R. Fuller Jr and C. V. Ciobanu, *Elastic Constants of B-Eucryptite Studied by Density Functional Theory*, Physical Review B **81**, 104106 (2010).
26. F. Tasnadi, I. A. Abrikosov and I. Katardjiev, *Significant Configurational Dependence of the Electromechanical Coupling Constant of B0.125al0.875n*, Applied Physics Letters **94** (2009).
10.1063/1.3119644
27. X. Yang, G. Zeng and W. Cao, *Analysis of Mechanical and Electrical Damages in Piezoelectric Ceramics*. (INTECH Open Access Publisher, 2010).

28. L. Egerton and D. M. Dillon, *Piezoelectric and Dielectric Properties of Ceramics in the System Potassium—Sodium Niobate*, Journal of the American Ceramic Society **42**, 438-442 (1959).
29. D. Yang, L. Wei, X. Chao, Z. Yang and X. Zhou, *First-Principles Calculation of the Effects of Li-Doping on the Structure and Piezoelectricity of (K_{0.5}Na_{0.5})NbO₃ Lead-Free Ceramics*, Physical Chemistry Chemical Physics **18**, 7702-7706 (2016).
30. Q.-M. Wang, X.-H. Du, B. Xu and L. E. Cross, *Electromechanical Coupling and Output Efficiency of Piezoelectric Bending Actuators*, IEEE transactions on ultrasonics, ferroelectrics, and frequency control **46**, 638-646 (1999).
31. M. Kim, J. Kim and W. Cao, *Aspect Ratio Dependence of Electromechanical Coupling Coefficient of Piezoelectric Resonators*, Applied Physics Letters **87**, 132901 (2005).
32. G. Wingqvist, *Thin-Film Electro-Acoustic Sensors Based on AlN and Its Alloys: Possibilities and Limitations*, Microsystem technologies **18**, 1213-1223 (2012).
33. K. Uchino, *Piezoelectric Ultrasonic Motors: Overview*, Smart materials and structures **7**, 273 (1998).
34. H. A. Sodano, D. J. Inman and G. Park, *A Review of Power Harvesting from Vibration Using Piezoelectric Materials*, Shock and Vibration Digest **36**, 197-206 (2004).
35. R. Turner, P. A. Fuierer, R. Newnham and T. Shrout, *Materials for High Temperature Acoustic and Vibration Sensors: A Review*, Applied acoustics **41**, 299-324 (1994).
36. K. Uchino, *Piezoelectric Actuators and Ultrasonic Motors*. (Springer Science & Business Media, 1996).
37. S. Baroni, S. De Gironcoli, A. Dal Corso and P. Giannozzi, *Phonons and Related Crystal Properties from Density-Functional Perturbation Theory*, Reviews of Modern Physics **73**, 515 (2001).
38. F. Bernardini, V. Fiorentini and D. Vanderbilt, *Polarization-Based Calculation of the Dielectric Tensor of Polar Crystals*, Physical review letters **79**, 3958 (1997).